Inorg. Chem. **2004**, *43*, 5961–5972

Theoretical Studies of Ground and Excited Electronic States in a Series of Rhenium(I) Bipyridine Complexes Containing Diarylethynyl-Based Structure

Li Yang,[†] Ai-Min Ren,[†] Ji-Kang Feng,*[,†,‡] Xiao-Dong Liu,[‡] Yu-Guang Ma,[§] and Hong-Xing Zhang[†]

State Key Laboratory of Theoretical and Computational Chemistry, Institute of Theoretical Chemstry, The College of Chemistry, and Key Laboratory for Supramolecular Structure and Materials of Ministry of Education, Jilin University, Changchun 130023, P. R. China

Received March 1, 2004

The photophysical properties, which vary as X is varied, of Re(I)–halide complexes (X_2-bpy)$Re^{I}Cl(CO)_3$ (where X= ph, DAE, DNE, and DPE; ph = phenyl (1); DAE = di(amineoethynylbenzene) (2); DPE = di(phenylethynylbenzene) (3); DNE = di(nitroethynylbenzene) (4); bpy=2,2′bipyridine), are investigated using density functional theory (DFT). The electronic properties of the neutral molecules, in addition to the positive and negative ions, are studied using B3LYP functional. Excited singlet and triplet states are examined using time-dependent density functional theory (TDDFT). The low-lying excited-state geometries are optimized at the ab initio configuration interaction singlets level. As shown, the diarylethynyl-based structure is an integral component of the bpy π-conjugated network, which results in a good planar structure. The occupied orbitals involved in the transitions have a significant mixture of metal Re and group Cl, and the lowest unoccupied orbital is a π^* orbital, which extends from ligand bpy to diarylethynyl-based substituents. The luminescence for each complex originates from the lowest triplet excited states and is assigned to the mixing of MLCT and LLCT characters. Significant insights on the effects of these diarylethynyl conjugated structure and ending substituents (NH_2, ph, and NO_2) on absorption and emission spectra are observed by analysis of the results of the TDDFT method. The diarylethynyl-based π-conjugated network makes both the absorption and emission spectra red-shifted compared with simple complex (bpy)$Re^{I}Cl(CO)_3$. Furthermore, an electron-releasing group (NH_2) makes absorption and emission spectra blue-shift and an electron-withdrawing group (NO_2) makes them red-shift.

Introduction

The photochemical and photophysical properties of diimine complexes with d^6 metal ions, such as rhenium(I), ruthenium(II), and osmium(II), are tremendously interesting from the standpoint of basic science as well as for their practical applications.[2−9] Rhenium diimine complexes of the type *fac*-$[Re^{(I)}(LL)(CO)_3(X)]^{n+}$ (n = 0,1; LL = diimine ligand) have been well studied because they are excellent emitters, photocatalysts, and building blocks for supramolecules.[10−13] An understanding of the photochemistry of transition metal compounds requires knowledge of the properties of molecular orbitals, spectra, and appropriate excited states. These spectroscopic and structural features are a big challenge to the interplay between theory and experiment and have

* To whom correspondence should be addressed. E-mail: Jikangf@yahoo.com. Fax: +86-431-8945942.
[†] State Key Laboratory of Theoretical and Computational Chemistry, Institute of Theoretical Chemstry.
[‡] The College of Chemistry.
[§] Key Laboratory for Supramolecular Structure and Materials of Ministry of Education.

(1) Yang, L.; Ren, A. M.; Feng, J. K. *J. Phys. Chem. A*, in press.
(2) Balk, R. W.; Stufkens, D. J.; Wrighton, M. S.; Morse, D. L. *J. Chem. Soc., Dalton Trans.* **1981**, 1124.
(3) Caspar, J. V.; Meyer, T. J. *J. Phys. Chem.* **1983**, *87*, 952.
(4) Dominey, R. N.; Hauser, B.; Hunham, J. *Inorg. Chem.* **1991**, *30*, 4754.
(5) George, M. W.; Johnso, F. P. A.; Westwell, J. R.; Hodges, P. M.; Turner, J. J. *J. Chem. Soc., Dalton Trans.* **1993**, 2977.
(6) Reitz, G. A.; Dressich, W. J. Demas, J. N.; DeGraff, B. A. *J. Am. Chem. Soc.* **1993**, *115*, 8230.
(7) Smothers, W. K.; Wrighton, M. S. *J. Am. Chem. Soc.* **1983**, *105*, 1067.
(8) Shinozaki, K.; Takahashi, N. *Inorg. Chem.* **1996**, *35*, 3917.
(9) Striplin, D. R.; Crosby, G. A. *Chem. Phys. Lett.* **1994**, *221*, 426.
(10) Oriskovich, T. A.; White, P. S.; Thorpe, H. H. *Inorg. Chem.* **1995**, *34*, 1629.
(11) Kotch, T. G.; Lees, A. J. *Chem. Mater.* **1992**, *3*, 25.
(12) Kotch, T. G.; Lees, A. J.; Fuerniss, S. J.; Papathomas, K. I.; Snyder, R. W. *Inorg. Chem.* **1993**, *32*, 2570.
(13) Thornton, N. B.; Schanze, K. S. *Inorg. Chem.* **1993**, *32*, 4994.

10.1021/ic049735l CCC: $27.50
Published on Web 08/19/2004

important implications for the spectroscopy and photochemistry of the broad and important class of low-valent metal complexes containing simultaneously electron-donating and electron-withdrawing substituent effects. Moreover, their photochemistry and photophysics represent a challenge to the understanding of excited-state dynamics. The main difficulties against a reliable computational approach are related to the size of such systems and to the presence of strong electron correlation effects. Both properties are difficult to treat in the framework of the quantum mechanical methods rooted in the Hartree−Fock (HF) theory.

On one hand, density functional theory (DFT) is successful at providing a means to evaluate a variety of ground-state properties with an accuracy close to that of post-HF methods.[14,15] In this context, remarkable structural predictions have been obtained especially using the "hybrid" density functionals[16,17] such as B3LYP and B3PW91 combining "exact exchange" with gradient-corrected density functionals. As a consequence, there is currently a great interest in extending DFT to excited electronic states.[18] The time-dependent DFT approach (TDDFT) offers a rigorous route to the calculation of vertical electronic excitation spectra.[19−21] Furthermore, applications of TDDFT approaches have recently been reported on transition metal complexes and get good results.[22−25] On the other hand, Gaussian offers the configuration interaction singlets (CIS) approach, modeling excited states as combinations of single substitutions out of the Hartree−Fock ground state.[26] When paired with a basis set, it also may be used to define excited-state model chemistries whose results may be compared across the full range of practical systems. Theoretical investigations on excited states are uncommon but necessary for the molecules used in organic light emitting diode devices (OLEDs), because the calculation of excited-state properties typically requires significantly more computational effort than is needed for the ground states.

Although there are many articles on photophysical properties of luminescent complexes, there are few theoretical studies on excited states and luminescent properties for d^6 metal complexes, especially for rhenium complexes. In this paper, the structure and electronic properties of the ground and lowest excited states for a family of metal bpy halide complexes containing the diarylethynyl-based π-conjugated network $(X_2\text{-bpy})ReCl(CO)_3$[27] have been simulated. We were particularly interested in understanding how expanding the ligand π system would affect orbital and transition character. We were similarly interested in understanding whether and how diarylethynyl-based π-conjugated properties would modulate orbital and transition character. On the other hand, we wanted to show the potential of a quantum mechanical modeling based on DFT, in the evaluation of ground- and excited-state properties by comparison to the available experimental data.

Computation Methods

Calculations on the electronic ground state of four related Re(I)−halide complexes $(X_2\text{-bpy})ReCl(CO)_3$ were carried out use B3LYP density functional theory. "Double-ξ" quality basis set LANL2DZ, which uses Duning D95V basis set on first row atoms, Los Alamos ECP plus DZ on Na−Bi, was employed as the basis set. A relativistic effective core potential (ECP) on Re replaced the inner core electrons leaving the outer core $[(5s^2)\ (5p^6)]$ electrons and the $(5d^6)$ valence electrons of Re(I). The excited-state geometries were optimized at the CIS level of theory. The transition energies will be calculated at the ground-state and excited-state geometries, and the results are compared with the available experimental data. The nature of the excited states, as well as the positive and negative ions with regard to "electron−hole" creation, is relevant to their use in OLED materials. The geometries were fully optimized with *Cs* symmetry constraints. All calculations are performed with Gaussian 03 software package using a spin-restricted formalism at the B3LYP/LanL2DZ level of theory, which has proved useful for other metal polypyridyl complexes.[28]

Results and Discussion

The four Re(I)−halide complexes $(X_2\text{-bpy})ReCl(CO)_3$ are shown as Figure 1. For the calculated ground-state geometries, the electronic structure is examined in terms of the highest occupied and lowest virtual molecular orbitals. The nature of the low-lying excited states is then explored using the TD-DFT approach to derive both absorption spectra and emission spectra, which are compared to available spectroscopic data.

Molecular Structures. Shown in Figure 2 are the molecular structures of complexes **1** and **2**, optimized by G03/B3LYP DFT calculations, and the selected bond lengths are summarized in Table 1. As depicted, the rhenium(I) in each case adopts a distorted octahedral coordination geometry, and the carbonyl groups are arranged in a facial orientation. Hereinafter, the CO ligands cis and trans to the bpy ligand are referred to as "axial" and "equatorial", respectively. Noticeably, as shown in Figure 2, complex **1** exhibits a distortion of 41.7(9)° between substituent phenyl and ligand bpy, which breaks a planar structure between them, whereas for complex **2**, the diarylethynyl unit is an integral component of the bpy π-conjugated network; that is, ethynyl spacers are capable of expanding the bipyridyl ligand (acceptor ligand) π system, which results in a good planar structure.

(14) Koch, W.; Holthausen, M. C. *A Chemist's Guide to Density Functional Theory*; Wiley-VCH: Weinheim, Germany, 2000.
(15) Adamo, C.; di Matteo, B. V. *Adv. Quantum Chem*. **1999**, *36*, 4.
(16) Lee, C.; Yang, W.; Parr, R. G. *Phys. Rev. B* **1998**, *37*, 785.
(17) Becke, A. D. *J. Chem. Phys*. **1993**, *98*, 5648.
(18) Runge, E.; Gross, E. K. *U. Phys. Rev. Lett*. **1996**, *76*, 1212.
(19) Bauernschmitt, R.; Ahlrichs, R. *Chem. Phys. Lett.* **1996**, *256*, 454.
(20) Casida, M. K.; Jamorski, C.; Casida, K. C.; Salahub, D. R. *J. Chem. Phys.* **1998**, *108*, 4439.
(21) Matsuzawa, N. N.; Ishitani. A.; Uda, T. *J. Phys. Chem. A* **2001**, *105*, 4953.
(22) Rosa, A.; Baerends, E. J.; vanGisbergen, S. J. A.; vanLenthe, E.; Gooeneveld, J. A.; Snihders, J. G. *J. Am. Chem. Soc*. **1999**. *121*, 10356.
(23) Adamo, C.; Bareone, V. *Theor. Chem. Acc*. **2000**, *105*, 169−172.
(24) Boulet, P.; Chermett, H.; Daul, C.; Gilardoni, F.; Rogemond, F.; Weber, J.; Zuber, G. *J. Phys. Chem. A* **2001**, *105*, 885−894.
(25) Farrell, I. R.; van Slageren, J.; Zalis, S.; Vlcek, A. *Inorg. Chim. Acta* **2001**, *315*, 44−52.
(26) Foresman, J. B.; Head-Gordon, M.; Pople, J. A. Frisch, M. J. *J. Phys. Chem*. **1996**, *100*, 9047.
(27) Walters, K. A.; Kim, Y. J.; Hupp, J. T. *Inorg. Chem.* **2002**, *41*, 2909−2919.
(28) Zheng, K. C.; Wang, J. P.; Peng, W. L.; Liu, X. W.; Yun, F. C. *J. Phys. Chem. A* **2001**, *105*, 10899.

Table 1. Selected Calculated Bond Lengths for Complexes **1**−**4**

	1		**2**		**3**		**4**	
bond distances (Å)	S_0	T_1	S_0	T_1	S_0	T_1	S_0	T_1
R[Re−N(1,1′)]	2.1682	2.1847	2.1673	2.1743	2.166	2.1934	2.1622	2.1995
R[Re−C(1,1′)]	1.9252	1.9572	1.9249	1.9603	1.9259	1.9578	1.9279	1.9566
R[Re−C(7)]	1.9094	1.9267	1.909	1.9261	1.9101	1.9272	1.9122	1.9276
R[Re−Cl]	2.5508	2.5714	2.5519	2.5723	2.5502	2.5695	2.5477	2.5674

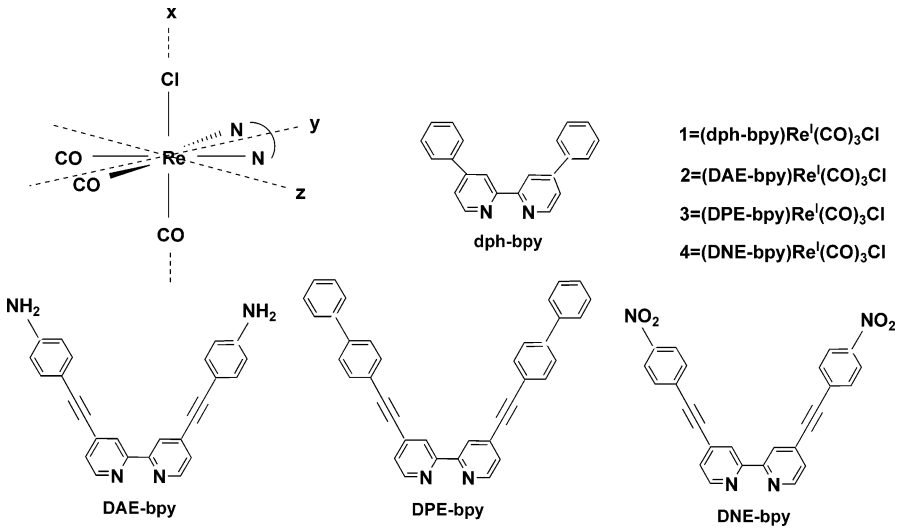

Figure 1. Schematic structures of complexes (X_2–bpy)Re(CO)$_3$Cl and the 4,4′-2X-bpy ligands used.

In fact, complexes **3** and **4** have similar geometrical rearrangements with complex **2** according to calculations. We noted that the axial M−CO_{ax} bond in the four complexes is always shorter than the equatorial M−CO_{eq} bonds. This is a manifestation of the competition for M → L back-bonding of ligands with a trans configuration in the transition metal complex. Because the chlorine group is a weak electron acceptor, the axial carbonyl ligand benefits from increased back-bonding to give a shorter and stronger M−CO_{ax} bond. Moreover, axial Re−Cl and Re−CO_{ax} bond lengths vary right about; in other words, the former becomes longer and the latter is shorter. Such as for complex **4**, the Re−C (7) bond is the longest among the four complexes and Re−Cl bond is the shortest among them.

Different structure makes the orbital character different, which will be discussed in the following section. Before proceeding further, a brief comment on the electron-donating, -withdrawing, or -delocalizing nature of each substituted bipyridine is in order. The phenyl-subsituted bipyridine complex **1** exhibits both electron-withdrawing and -delocalizing effects. The addition of ethynyl spacers is anticipated to amplify both of these effects. Complex **3** is clearly more strongly withdrawing than **2**. And for **4**, the substituents are strongly electron withdrawing. The Re−N bond lengths in arylethynyl complexes **2**−**4** are shorter than that in complex **1**. Furthermore, for complexes **2**−**4**, ending substituents (NH_2, ph, NO_2) influence the molecular structure through the diarylethynyl-based π-conjugated network. With the increasing withdrawing ability NH_2 < ph < NO_2, Re−N bond lengths decrease (2.1673 > 2.166 > 2.1622 Å), axial Re−CO_{ax} (1.909 < 1.9101 < 1.9122 Å) increase, and Re−Cl decrease (2.5519 > 2.5502 > 2.5477 Å); and the equatorial M−CO_{eq} bond lengths increase (1.9249 < 1.9259 < 1.9279 Å) in the order given.

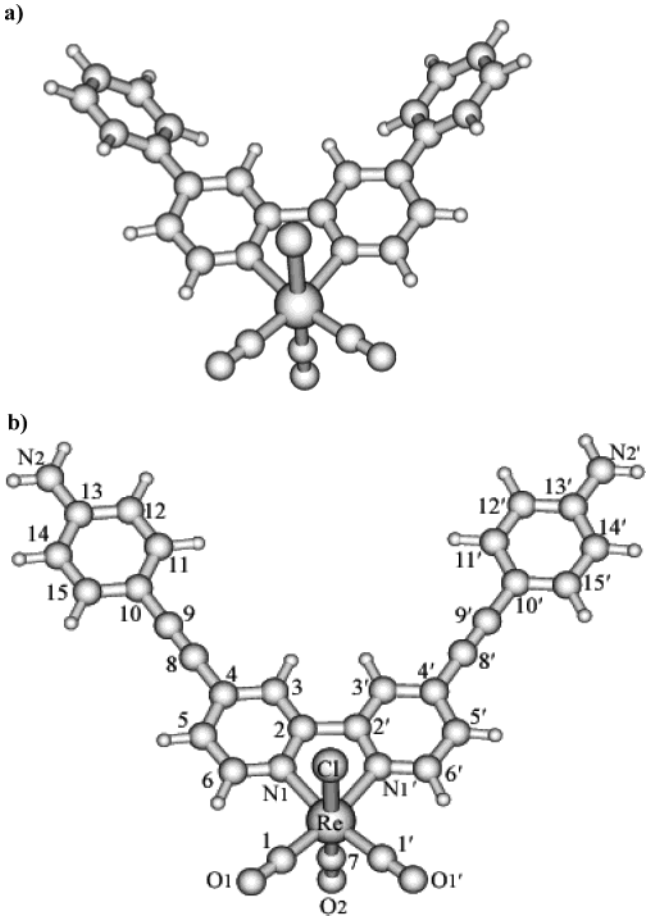

Figure 2. Calculated structures for molecule (a) (dph-bpy)ReCl(CO)$_3$ (**1**) and (b) (DAE-bpy)ReCl(CO)$_3$ (**2**).

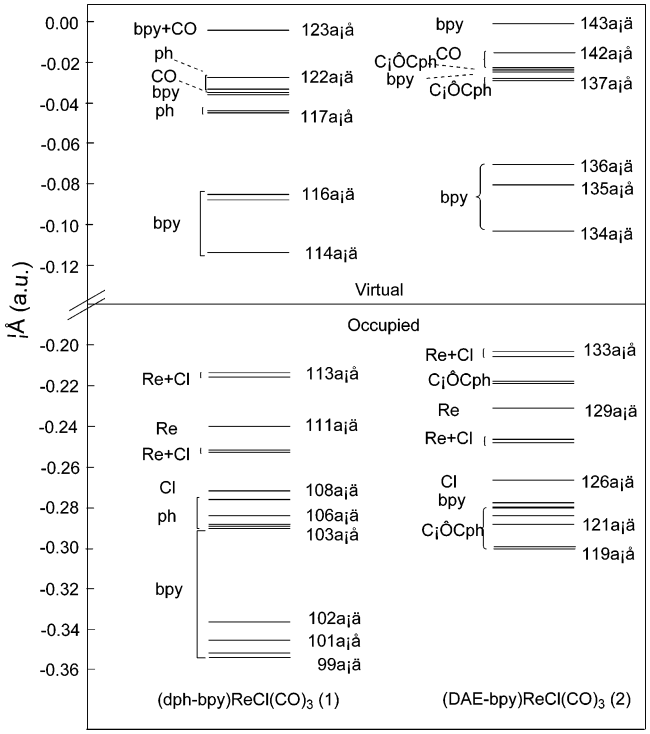

Figure 3. Energy level diagram of frontier molecular orbitals calculated at the B3LYP/LanL2DZ level for complexes (dph-bpy)ReCl(CO)$_3$ (**1**) and (DAE-bpy)ReCl(CO)$_3$ (**2**). Labels on the left denote the dominant moiety contributing to each molecular orbital. For clarity, only a few of the molecular orbitals are numbered.

Molecular Orbitals. It will be useful to examine the highest occupied and lowest virtual orbitals for these Re complexes to provide the framework for the excited-state TDDFT and CIS calculations in the subsequent section. Moreover, frontier orbitals play a relevant role in such systems, because they rule the electronic excitations and the transition character. The frontier orbitals (15 occupied MOs and 10 virtual MOs) are plotted according to their energies in Figure 3 for complexes **1** and **2** as an example to determine the effect of the arylethynyl spacer. The assignment of the type of each MO was made on the basis of its composition (see Table 2, in which only the most important five occupied and three virtual (unoccupied) orbitals are listed, together with orbital compositions expressed in terms of contributions from the Re central atom, axial group Cl, CO ligands, arylethynyl groups and ending substituents, and then bpy ligand and by visual inspection of its three-dimensional representation (e.g., Figure 4).

As plotted, a diarylethynyl-based group increases the energies of both occupied and virtual orbitals. The two highest occupied orbitals (HOMOs) and three lowest virtual orbitals (LUMOs) have similar compositions for the two molecules. Whereas, some lower-energy occupied MOs are mainly centered on the bpy ligands for complex **1** and they extend to a diarylethynyl-based group for complex **2**. Similarly, the higher LUMOs extend to a diarylethynyl-based group for complex **2**, although they show different compositions in different complexes. However, since the contribution from these orbitals is quite small for low-energy transition, we only concentrate on the orbitals listed in Table 2.

Table 2. Calculated Highest Occupied and Lowest Virtual Orbitals with Character for the Four Re Complexes[a]

		composition(%)						
orbital	energy (au)	Re	bpy	CO	Cl	c≡cph	ph(NH_2, NO_2)	character
				(dph-bpy)Re(CO)$_3$Cl				
occupied								
109 a″	-0.253	26	16	14	37		7	Cl
110 a′	-0.252	24	16	18	37		11	Cl
111 a′	-0.239	64	3	32	0		0	Re
112 a′	-0.215	37	8	18	37		1	Re + Cl
113a″	**-0.212**	**37**	**5**	**22**	**35**		**0**	**Re + Cl**
				ΔE_1(HOMO − LUMO) = 0.101				
virtual								
114 a′	**-0.110**	**2**	**82**	**4**	**2**		**11**	**bpy**
115 a″	-0.084	0	67	1	0		32	bpy
116 a′	-0.081	0	86	0	0		13	bpy
				(DAE-bpy)Re(CO)$_3$Cl				
occupied								
129 a′	-0.231	64	3	33	0	0	0	Re
130 a′	-0.218	1	10	1	12	53	22	c≡cph
131 a″	-0.218	0	10	0	6	59	25	c≡cph
132 a′	-0.204	35	7	18	30	7	2	Re + Cl
133 a″	**-0.203**	**36**	**5**	**21**	**33**	**37**	**1**	**Re + Cl**
				ΔE_2(HOMO − LUMO) = 0.100				
virtual								
134 a′	**-0.103**	**2**	**76**	**4**	**2**	**15**	**2**	**bpy**
135 a″	-0.081	0	63	1	0	33	32	bpy
136 a′	-0.072	0	89	1	0	10	1	bpy
				(DPE -bpy)Re(CO)$_3$Cl				
occupied								
161 a′	-0.239	54	5	27	1	9	5	Re
162 a″	-0.239	1	11	1	7	52	28	c≡cph
163 a′	-0.238	14	10	8	10	38	19	c≡cph
164 a′	-0.214	36	8	18	35	2	0	Re + Cl
165 a″	**-0.211**	**37**	**5**	**21**	**35**	**1**	**0**	**Re + Cl**
				ΔE_3(HOMO − LUMO) = 0.095				
virtual								
166 a′	**-0.116**	**3**	**72**	**4**	**2**	**18**	**2**	**bpy**
167 a″	-0.097	0	52	1	0	40	7	bpy
168 a′	-0.085	0	82	0	0	18	3	bpy
				(DNE -bpy)Re(CO)$_3$Cl				
occupied								
143 a″	-0.268	25	15	13	37	11	1	Cl + Re
144 a′	-0.267	22	16	13	33	16	1	Re + Cl
145 a′	-0.255	64	3	32	0	0	0	Re
146 a′	-0.230	36	8	18	37	1	0	Re + Cl
147 a″	**-0.228**	**37**	**5**	**21**	**36**	**1**	**0**	**Re + Cl**
				ΔE_4(HOMO − LUMO) = 0.079				
virtual								
148 a′	**-0.149**	**2**	**28**	**2**	**1**	**32**	**35**	**c≡cph + ph + bpy**
149 a″	-0.145	0	11	0	0	37	51	ph + c≡cph
150 a′	-0.125	1	57	2	1	11	28	bpy

[a] ΔE refers to the energy gap.

It can be seen from Table 2 that a diarylethynyl-based group decreases the energy gaps, which also shows that diarylethynyl-based groups in complexes **2**−**4** extend the conjugated system and in contour plots (Figure 4), the π-conjugated planar network consisting of bpy and diarylethynyl is clear. Importantly, ending substituents have profound effects on energy gaps. With the increasing withdrawing ability, NH_2 < ph < NO_2, energy gaps decrease in the order $|\Delta E_2|$ (0.100 au) > $|\Delta E_3|$(0.095 au) > $|\Delta E_4|$-(0.079 au), which is the same that simple electron-releasing and -withdrawing substituted complexes do.[1]

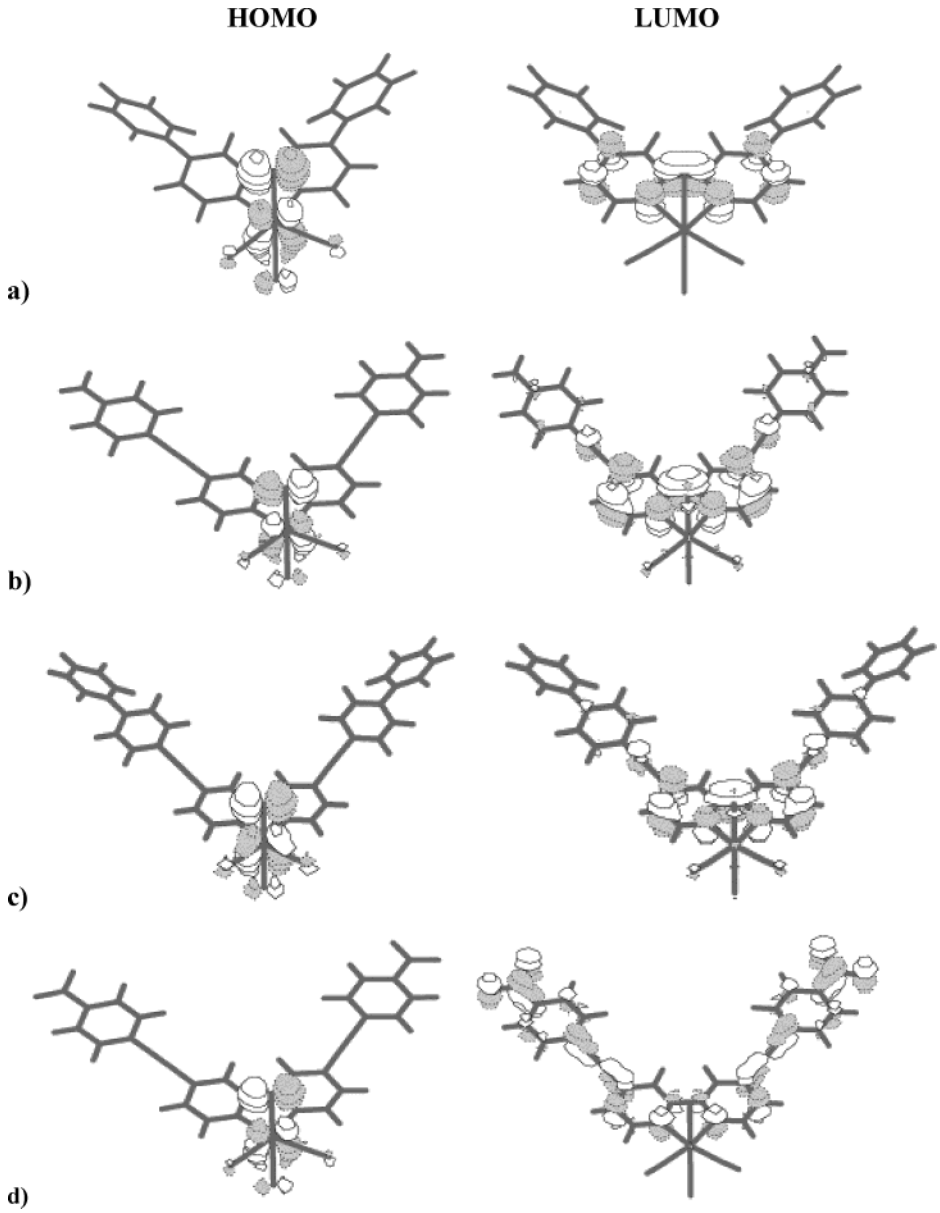

Figure 4. Contour plots of highest occupied and lowest virtual orbitals in considered molecules (a) (dph-bpy)$ReCl(CO)_3$, (b) (DAE-bpy)$ReCl(CO)_3$, (c) (DPE-bpy)$ReCl(CO)_3$, and (d) (DNE-bpy)$ReCl(CO)_3$.

At the same time, these data illustrate the profound effects that ending substituent changes at the bpy ligand have on the frontier orbital properties of the complexes. In all four complexes, the two highest occupied orbitals have different symmetries, HOMO (a″) and $HOMO_{-1}$ (a′), which are both a mixture of rhenium and chlorine orbital character. In other words, the HOMO, a a″orbital, is composed mainly of chloride p_z orbitals that form antibonding interactions with metal d_{xz} orbitals (Figure 4a). There seems to be some deviations from the experimental conclusion; that is, experiment stressed more the contribution of metal than calculation. On one hand, Turki and the co-workers[29] calculated the UV−visible absorption spectra of Ru complex containing Cl with CASSCF/CASPT2 and TD-DFT methods. They thought DFT calculations overestimate halide contributions in metal−halide complexes, especially if a low-valent metal atom is involved, although DFT approaches are remarkably good in the case of non-halide complexes. On the other hand, Stufkens et al.[30,31] have noted that the electronic transitions to the α-diimine have strongly mixed MLCT/LLCT character due to the interaction of $M-d_\pi$ and $X-p_\pi$ orbitals in the experiment. As a result, two absorption bands are observed, the relative intensities of which depend on the metal character of the orbitals involved in the transitions.

For electron-releasing substituent (NH_2)-substituted complex **2** and phenyl-substituted complex **3**, $HOMO_{-2}$ and $HOMO_{-3}$ are predominantly diarylethynyl π character (∼50%), with a significant admixture of ending subsituent

(29) Turki, M.; Daniel, C.; Záliš, S.; Vlček, A., Jr.; van Stageren, J.; Stufkens, D. J. *J. Am. Chem. Soc*. **2001**, *123*, 11431−11440.

(30) Stufkens, D. J.; Vlček, A., Jr. *Coord. Chem. Rev.* **1998**, *177*, 127.

(31) Nieuwenhuis, H. A.; Stufkens, D. J.; McNicholl, R.-A.; Al-Obaidi, A. H. R.; Coates, C. G.; Bell, S. E. J.; McGarvey, J. J.; Westwell, J. George, M. W. Turner, J. J. *J. Am. Chem. Soc*. **1995**, *117*, 5579−5585.

Table 3. Ionization Potentials, Electron Affinities, and Spin Densities for the Four Complexes

		spin density of cation (%)								
compds	IP (eV)	Re	bpy	3CO	Cl	2ph	(C≡Cph,	NH_2,	ph,	NO_2)
1	7.33	0.52	0.02	0.10	0.31	0.05				
2	6.67	0.39	0.03	0.05	0.15		0.23	0.15		
3	7.10	0.44	0.06	0.07	0.16		0.17		0.10	
4	7.75	0.46	0.04	0.10	0.21		0.19			0.00
		spin density of anion (%)								
compds	*E* (eV)	Re	bpy	3CO	Cl	2ph	(C≡Cph,	NH_2,	ph,	NO_2)
1	-1.76	-0.01	0.83	0.03	0.02	0.13				
2	-1.68	-0.02	0.78	0.05	0.02		0.16	0.01		
3	-2.06	-0.01	0.60	0.03	0.00		0.30		0.07	
4	-3.04	-0.01	0.40	0.03	0.01		0.28			0.27

p_x orbitals of nitrogen on NH_2 or p_x orbital of carbon on the ph ring (~20%). The a′ $HOMO_{-4}$ for complexes **2** and **3** is strongly delocalized over metal Re (~50−60%), having nearly 30% contribution CO_{eq}.

The three highest LUMOs for **2** and **3** are calculated to be almost exclusively located on diimine bpy (over 70%), except for $LUMO_{+1}$, in which a significant contribution comes from diarylethynyl (over 30%).

Comparing **4** to **2** and **3**, the $HOMO_{-2}$ (a′) is dominant metal d character (over 60%), and $HOMO_{-3}$ (a′) and $HOMO_{-4}$ (a″) are formed by the contributions from all fragments, with the major ones coming from both the chlorine and metal Re. With the influences of strong electron-withdrawing substituent NO_2, LUMO (a′) and $LUMO_{+1}$ (a″) are mainly located on ending substituent NO_2 (35−50%), having π-bonding character with 30% contribution of diarylethynyl (Figure 4c), and $LUMO_{+2}$ having a′ symmetry is mainly characterized π^* located on bpy, with considerable contribution from NO_2.

In the contour plots, the mixing of 5d and group Cl p character is evident for each complex. While the LUMO is mainly located on bpy for **1** and **3** and for **4**, the electron extends through to ethyne and benzene until NO_2. Thus, there must be an admixture between MLCT and LLCT at the transition from ground state to excited state.

Ionization Potentials and Electron Affinities. Additional information derived from our calculations provides insight into the interrelationship of structure and electronic behavior, in particular the response of the molecule to the formation of a hole or the addition of an electron. Table 3 contains the ionization potentials (IPs), electron affinities (EAs), and spin density. The IP is obtained by differences in the total self-consistent energies of the cation and the neutral ground state and similarly for the EA. In all cases, the energy required to create a hole is ~7 eV, while the extraction of an electron from the anion requires ~2 eV. In fact, early work has amply demonstrated that $ReX(CO)_3(\alpha$-diimine) complexes are both strong reductants and oxidants. Experimental research reveals nearly reversible oxidation and reduction waves at ~+1.3 and ~-1.3 V versus an aqueous SCE for the complex *fac*-$ReCl(CO)_3$(phen).[32] It is found that the calculated IP values increase with increasing withdrawing ability (6.67 < 7.10 < 7.75 eV) for complexes **2**−**4**. These all correspond to removal of an electron from the "5d" orbital. As shown in the cation spin densities in the Table 3, over 40% of the spin density is on the Re and the proportion increases with increasing electron-withdrawing ability (0.39 < 0.44 < 0.46). The remainder relatively large proportion shares on the diarylethynyl group and relatively less on Cl for **2**, **3,** and **4**. The distribution agrees well with the analysis for HOMO.

Four complexes show weakly bound negative ions, corresponding to the electron affinity. On the contrary, with IP, the EA values decrease with increasing electron-withdrawing ability (−1.68 > −2.06 > −3.04 eV) going from **2** to **4.** The unpaired spin densities are largely on bpy ligands, and contrary to cation spin density, the proportion decreases with increasing electron-withdrawing ability (0.78 > 0.44 > 0.46). For **2** and **3**, the remainder largely shares on the diarylethynyl, and for **4**, besides some sharing on diarylethynyl, a considerable percentage is on ending substituent NO_2 due to the strong electron-withdrawing ability, which is consistent with the analysis of LUMO.

Excitation Energies. TDDFT calculations are employed to examine the low-lying singlet and triplet excited states of the Re complexes. Selected singlet excited states with the greatest oscillator strengths are displayed in Tables 4−7, respectively. The energy of each excited is vertical excitation energy in electronvolts from the ground state.

An experimentally used model of an excited state corresponds to excitation of an electron from an occupied to a virtual MO (i.e., a one-electron picture). However, the excited states calculated herein demonstrate that excited-state electronic structures are best described in terms of multiconfigurations, wherein a linear combination of several occupied-to-virtual MO excitations comprises a given optical transition. Assignment of the character of each excited state was based on the compositions of the occupied and virtual MOs of the dominant configuration(s) for that excited state. Such as for complex **2**, for S_{13}(A″) excited state, the dominant excitation is 129 → 135, and since the occupied orbital (129) is metal-based and the virtual orbital (135) is bipyridine/diarylethynyl π^*, the transition is designated a metal-to-ligand charge transfer (MLCT). Similarly, for S_{15}(A″) excited state, the dominant excitation is 131 → 136, and since the occupied orbital (131) is localized on a diarylethynyl moiety and virtual orbital (136) type is bipyridine π^*, the transition is

(32) Luong, J. C.; Nadjo, L.; Wrighton, M. S. *J. Am. Chem. Soc.* **1978**, *100*, 5790.

Table 4. Selected Calculated Excitation Energies (E), Wavelengths (λ), Oscillator Strenghs (×c4), and Dominant Excitation Character for Low-Lying Singlet (S_n) and Triplet (T_n) States of Complex (dph-bpy)ReCl(CO)$_3$

state	excitation	E_{cal}, eV	λ_{cal}, nm	×c4$_{cal}$	$\lambda_{expt.}$, nm	character
			Singlet Excited States			
1(A″)	113 → 114(0.70)	2.03	609	0.0039		Re/Cl → bpy (MLCT/LLCT)
9(A′)	110 → 114(0.66)	3.26	380	0.1749		Cl/Re → bpy (MLCT/LLCT)
					396(CH_2Cl_2)[27]	
					384(CH_2CN)[34]	
19(A″)	107 → 114(0.51)	4.06	305	0.1784		ph → bpy (LLCT)
	110 → 115(0.13)					Cl/Re → bpy (MLCT/LLCT)
20(A′)	110 → 116(0.53)	4.08	304	0.1817		Cl/Re → bpy (MLCT/LLCT)
	109 → 115(0.40)					Cl/Re → bpy (MLCT/LLCT)
28(A″)	103 → 114(0.49)	4.38	283	0.3095		bpy → bpy (IL)
	105 → 114(0.21)					ph → bpy (LLCT)
	112 → 117(0.21)					Cl/Re → bpy (MLCT/LLCT)
38(A″)	107 → 116(0.61)	4.77	260	0.2631		ph → bpy (LLCT)
	106 → 115(0.25)					ph → bpy (LLCT)
			Triplet Excited States			
1(A″)	113 → 114(0.71)	1.97	629	0.0000		Re/Cl → bpy (MLCT/LLCT)
2(A′)	112 → 114(0.71)	2.03	612	0.0000		Re/Cl → bpy (MLCT/LLCT)
3(A′)	111 → 114(0.70)	2.71	458	0.0000		Re → bpy (MLCT)
4(A″)	109 → 114(0.48)	2.74	453	0.0000		Cl/Re → bpy (MLCT/LLCT)
	112 → 115(0.31)					Re/Cl → bpy (MLCT/LLCT)
5(A′)	113 → 115(0.50)	2.80	443	0.0000		Re/Cl → bpy (MLCT/LLCT)
	112 → 116(0.21)					Re/Cl → bpy (MLCT/LLCT)

Table 5. Selected Calculated Excitation Energies (E), Wavelengths (λ), Oscillator Strenghs (×c4), and Dominant Excitation Character for Low-Lying Singlet (S_n) and Triplet (T_n) States of Complex (DAE-bpy)ReCl(CO)$_3$

state	excitation	$E_{cal.}$, eV	$\lambda_{cal.}$, nm	×c4$_{cal.}$	$\lambda_{expt.}$, nm	character
			Singlet Excited States			
1(A″)	133 → 134(0.69)	2.02	613	0.0122		Re/Cl → bpy (MLCT/LLCT)
6(A″)	132 → 135(0.53)	2.83	438	0.2495		Re/Cl → bpy (MLCT/LLCT)
	131 → 134(0.41)					C≡Cph/NH_2 → bpy (LLCT)
7(A′)	130 → 134(0.57)	3.13	396	0.3166		C≡Cph/NH_2 → bpy (LLCT)
	133 → 135(0.28)					Re/Cl → bpy (MLCT/LLCT)
					408(CH_2Cl_2)[27]	
8(A″)	133 → 136(0.70)	3.23	384	0.0260		Re/Cl → bpy (MLCT/LLCT)
11(A′)	127 → 134(0.64)	3.41	364	0.1297		Re/Cl → bpy (MLCT/LLCT)
	128 → 135(0.10)					Re/Cl → bpy (MLCT/LLCT)
12(A″)	130 → 135(0.64)	3.44	360	0.4034		C≡Cph/NH_2 → bpy (LLCT)
	131 → 136(0.14)					C≡Cph/NH_2 → bpy (LLCT)
13(A″)	129 → 135(0.69)	3.49	356	0.0108		Re → bpy (MLCT)
15(A″)	131 → 136(0.66)	3.59	346	0.2773		C≡Cph/NH_2 → bpy (LLCT)
16(A′)	130 → 136(0.46)	3.66	339	0.8477		C≡Cph/NH_2 → bpy (LLCT)
	131 → 135(0.40)					C≡Cph/NH_2 → bpy (LLCT)
31(A″)	125 → 134(0.33)	4.40	282	0.1181		bpy → bpy (IL)
	122 → 134(0.27)					C≡Cph/bpy → bpy (LLCT)
	128 → 136(0.19)					Re/Cl → bpy (MLCT/LLCT)
			Triplet Excited States			
1(A″)	133 → 134(0.70)	1.95	636	0.0000		Re/Cl → bpy (MLCT/LLCT)
2(A′)	132 → 134(0.71)	1.99	623	0.0000		Re/Cl → bpy (MLCT/LLCT)
3(A″)	131 → 134(0.60)	2.32	535	0.0000		C≡Cph/NH_2 → bpy (LLCT)
	130 → 135(0.29)					C≡Cph/NH_2 → bpy (LLCT)
4(A′)	130 → 134(0.62)	2.33	531	0.0000		C≡Cph/NH_2 → bpy (LLCT)
	131 → 135(0.30)					C≡Cph/NH_2 → bpy (LLCT)
5(A′)	129 → 134(0.69)	2.71	458	0.0000		Re → bpy (MLCT)

designated a ligand-to-ligand charge-transfer LLCT. Whereas for S_8 (A″), the dominant excitation is from 133 having a mixture of metal and chlorine orbital character to 136 with bipyridine π^* character and has been termed a mixed MLCT/LLCT character. Figure 5 illustrates the difference between MLCT and LLCT excitations for two strongly allowed transitions (Figure 5a and b) of **2**. Moreover, for S_1 excited state, the calculated spin density of positive and negative ion also has significant referenced value for transition assignment. For the majority of the excited states under investigation, most of the significant excited states exhibit mixed MLCT/LLCT character and, sometimes, intraligand transition (IL), as shown in Tables 4-7.

From Tables 5−7, it can be seen that consistent with the variation rules of the energy gaps, with the increasing electron-withdrawing ability of the substituents, the absorption bands exhibit red-shifts. For S_1, 2.02 (NH_2) > 1.92 (ph) > 1.64 eV (NO_2). In fact, excited-state character as a function of the molecular structure has been reviewed form the experimental point of view, such as in the literature,[29] the author addressed that the character of the lowest excited states changes gradually from MLCT to LLCT while halide ligand changes from Cl to Br, especially, to I in Re(E)(CO)$_3$(α-diimine) complexes.

The 35 lowest-energy triplet excited states were also calculated, using analogous TD-DFT methodology. The first

Table 6. Selected Calculated Excitation Energies (E), Wavelengths (λ), Oscillator Strenghs (×c4), and Dominant Excitation Character for Low-Lying Singlet (S_n) and Triplet (T_n) States of Complex (DPE-bpy)ReCl(CO)$_3$

state	excitation	$E_{cal.}$, eV	$\lambda_{cal.}$, nm	×c4$_{cal.}$	$\lambda_{expt.}$, nm	character
			Singlet Excited States			
1(A″)	165 → 166(0.70)	1.92	647	0.0117		Re/Cl → bpy (MLCT/LLCT)
8(A″)	162 → 166(0.62)	2.95	420	0.2551		C≡Cph/ph → bpy (LLCT)
	160 → 166(0.29)					Re/Cl → bpy (MLCT/LLCT)
9(A′)	163 → 166(0.57)	2.99	414	0.5042		C≡Cph/ph → bpy (LLCT)
	159 → 166(0.18)					Re/Cl → bpy (MLCT/LLCT)
					410(CH_2Cl_2)[27]	
10(A″)	160 → 166(0.63)	3.20	388	0.1658		Re/Cl → bpy (MLCT/LLCT)
13(A″)	163 → 167(0.59)	3.46	358	0.5573		C≡Cph/ph → b py/C≡Cph (LLCT)
	159 → 167(0.13)					Re/Cl → bpy/C≡Cph (MLCT/LLCT)
14(A′)	162 → 167(0.65)	3.57	347	0.8120		C≡Cph/ph → bpy/C≡Cph (LLCT)
18(A′)	163 → 168(0.48)	3.76	330	0.2543		C≡Cph/ph → bpy (LLCT)
	156 → 166(0.35)					Cl/CO → bpy (LLCT)
30(A″)	160 → 168(0.56)	4.08	304	0.1095		Re/Cl → bpy (MLCT/LLCT)
	151 → 166(0.21)					Cl/CO → bpy (LLCT)
31(A″)	155 → 166(0.56)	4.13	300	0.1045		Cl/CO → bpy (LLCT)
	160 → 168(0.30)					Re/Cl → bpy (MLCT/LLCT)
35(A′)	152 → 166(0.63)	4.25	292	0.1338		CO → bpy (LLCT)
	159 → 168(0.18)					Re/Cl → bpy (MLCT/LLCT)
38(A″)	151 → 166(0.48)	4.35	285	0.1100		Cl/CO → bpy (LLCT)
	155 → 166(0.32)					Cl/CO → bpy (LLCT)
			Triplet Excited States			
1(A″)	165 → 166(0.70)	1.85	671	0.0000		Re/Cl → bpy (MLCT/LLCT)
2(A′)	164 → 166(0.71)	1.90	654	0.0000		Re/Cl → bpy (MLCT/LLCT)
3(A″)	162 → 166(0.51)	2.38	522	0.0000		C≡Cph/ph → bpy (LLCT)
	163 → 167(0.31)					C≡Cph/ph → bpy/C≡Cph (LLCT)
4(A′)	163 → 166(0.49)	2.40	517	0.0000		C≡Cph/ph → bpy (LLCT)
	162 → 167(0.33)					C≡Cph/ph → bpy/C≡Cph (LLCT)
5(A′)	165 → 167(0.62)	2.58	481	0.0000		Re/Cl → bpy/C≡Cph (LLCT)
	163 → 166(0.30)					C≡Cph/ph → bpy (LLCT)

Table 7. Selected Calculated Excitation Energies (E), Wavelengths (λ), Oscillator Strenghs (×c4), and Dominant Excitation Character for Low-Lying Singlet (S_n) and Triplet (T_n) States of Complex (DNE-bpy) ReCl(CO)$_3$

state	excitation	$E_{cal.}$, eV	$\lambda_{cal.}$, nm	×c4$_{cal.}$	λ_{expt}, nm	character
			Singlet Excited States			
1(A″)	147 → 148(0.66)	1.64	754	0.0118		Re/Cl → NO_2/C≡Cph (MLCT/LLCT)
	147 → 150(0.25)					Re/Cl → bpy/NO_2 (MLCT/LLCT)
12(A′)	144 → 148(0.41)	2.90	428	0.1161		Re/Cl → NO_2/C≡Cph (MLCT/LLCT)
	147 → 151(0.37)					Re/Cl → NO_2/C≡Cph (MLCT/LLCT)
					422(CH_2Cl_2)[27]	
15(A″)	144 →149(0.69)	3.03	410	0.1868		Re/Cl → NO_2/C≡Cph (MLCT/LLCT)
17(A′)	143 → 149(0.62)	3.10	400	0.3647		Re/Cl → NO_2/C°Cph (MLCT/LLCT)
	144 → 148(0.23)					Re/Cl → NO_2/C°Cph (MLCT/LLCT)
23(A″)	141 → 148(0.63)	3.53	351	0.3698		C°Cph → NO_2/C°Cph (LLCT)
	143 → 150(0.16)					Re/Cl → bpy/NO_2 (MLCT/LLCT)
30(A″)	140 → 149(0.60)	3.82	324	0.1721		C°Cph → NO_2/C°Cph (LLCT)
	139 → 148(0.26)					bpy → NO_2/C°Cph (LLCT)
31(A′)	141 → 149(0.46)	3.82	324	0.7199		C°Cph → NO_2/C°Cph (LLCT)
	140 → 148(0.41)					C°Cph → NO_2/C°Cph (LLCT)
39(A′)	143 → 151(0.37)	4.04	307	0.1012		Re/Cl → NO_2/bpy (MLCT/LLCT)
	142 → 150(0.36)					Cl/CO → bpy/NO_2 (LLCT)
			Triplet Excited States			
1(A″)	147 → 148(0.65)	1.59	781	0.0000		Re/Cl → NO_2/C≡Cph (MLCT/LLCT)
	147 → 150(0.27)					Re/Cl → bpy/NO_2 (MLCT/LLCT)
2(A′)	146 → 148(0.66)	1.64	755	0.0000		Re/Cl → NO_2/C≡Cph (MLCT/LLCT)
	146 → 150(0.28)					Re/Cl → bpy/NO_2 (MLCT/LLCT)
3(A′)	147 → 149(0.69)	1.91	648	0.0000		Re/Cl → NO_2/C≡Cph (MLCT/LLCT)
4(A″)	146 → 149(0.69)	1.97	629	0.0000		Re/Cl → NO_2/C≡Cph (MLCT/LLCT)
5(A″)	147 → 150(0.64)	2.27	545	0.0000		Re/Cl → bpy/NO_2 (MLCT/LLCT)
	147 → 148(0.27)					Re/Cl → NO_2/C≡Cph (MLCT/LLCT)

five triplet excited states are listed in Table 2. MLCT, LLCT, and mixed MLCT/LLCT excited states are all seen, but most of them are the mixed-character excited states, as with the singlets. As expected from Hund's rule, transitions to the triplet states tend to be lower in energy than their corresponding singlets. For example, for complex **2**, the first triplet vertical transition energy is 1.95 eV lower than that of the first singlet excited state (2.02 eV), where both represent (predominantly) a MO 133 → MO 134 transition. The TDDFT results do not provide information on triplet−singlet absorption intensities since spin−orbit coupling effects are not included in current TDDFT approaches, which is why the oscillator strengthes are all zero for triplet excited states. Spin−orbit coupling can mix singlet and triplet states,

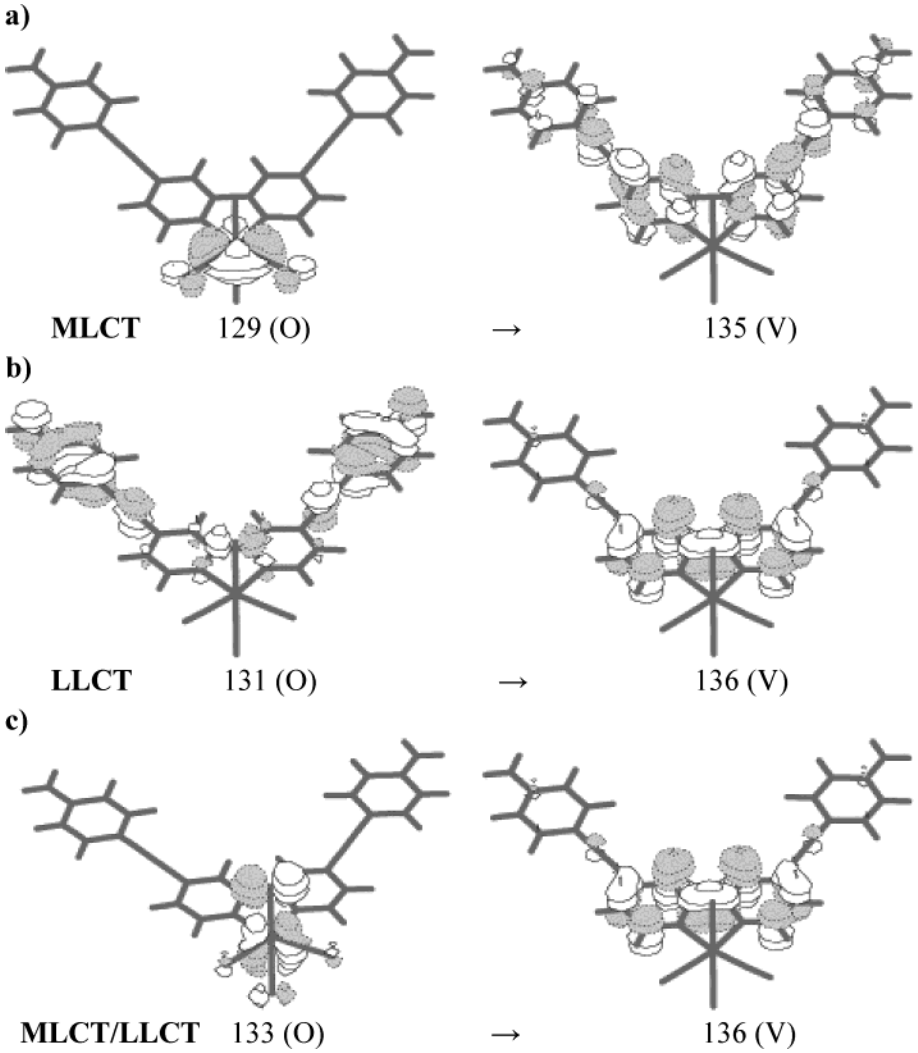

Figure 5. Example of dominant occupied and virtual orbitals for three different types of excitations of complex **2**. (a) Metal-to-ligand charge transfer (MLCT) excitation (129 → 135). (b) Ligand-to-ligand charge transfer (LLCT) excitation (131 → 136). (c) Mixed charge-transfer MLCT/LLCT excitation (133 → 136).

allowing the latter to acquire intensity in both absorption and emission. A second effect is that the triplet energies are shifted through coupling with higher singlet (or other triplet) states. For third row transition metals, one[33] estimates the lowest triplet states to be lower by ~0.2−0.3 eV from interactions with higher states through spin−orbital coupling. The TDDFT results should still provide a reasonable description of the overall orbital excitations that would be coupled in a subsequent spin−orbit treatment.

Comparison with Experimental Results. Combined with experimental data gathered over time, computed spectra may provide a reference for monitoring the behavior and possible degradation of the organic material in the device. The results of the TDDFT calculations for all four considered complexes are compared with experimental absorption data (see Tables 4−7). The spectral assignment is based on a comparison of experimental band maximums with calculated energies of transitions with significant oscillator strengths.

Compared to simple electron-releasing/-withdrawing substituted complexes, an expanding conjugated structure makes low-energy absorption bands red-shift about 30−50 nm,[1] such as $\lambda_{max} = 370$ nm for (bpy)ReCl(CO)$_3$. For complexes **2** and **3**, the low-energy absorption in an experiment at 408 and 410 nm similarly mainly corresponds to the calculated π (diarylethynyl) → π^* (bpy) (LLCT) excitation arising from $S_7(A')$ at 3.13 eV and $S_9(A')$ at 2.99 eV, respectively, both having significant d (Re)/p(Cl) → π^* (bpy) (MLCT/LLCT) character. The most intense calculated absorption peaks at 339 nm (3.66 eV) and at 347 nm (3.57 eV) arising from singlet state $S_{16}(A')$ and $S_{14}(A')$, respectively, are both mainly assigned to π (diarylethynyl) → π^*(bpy) (LLCT).

For complex **1**, the low-energy band at 396 nm occurs in the same region of a singlet-state $S_9(A')$ calculated at 3.26 eV, which arises from an admixture of p(Cl) → π^*(bpy) (LLCT) and d(Re) → π^* (bpy) (MLCT). The most intense absorption peak at 304 nm (4.08 eV) also arises from an admixture of p(Cl) → π^*(bpy) (LLCT) and d(Re) → π^* (bpy) (MLCT) of $S_{20}(A')$.

Noticeably, due to the effect of the strong electron-withdrawing ending substituent NO_2, the low-energy band at 422 nm corresponds to $S_{12}(A')$ which arises from an

(33) Jeffrey, H. P. *J. Phys. Chem. A* **2002**, *106*, 1634.

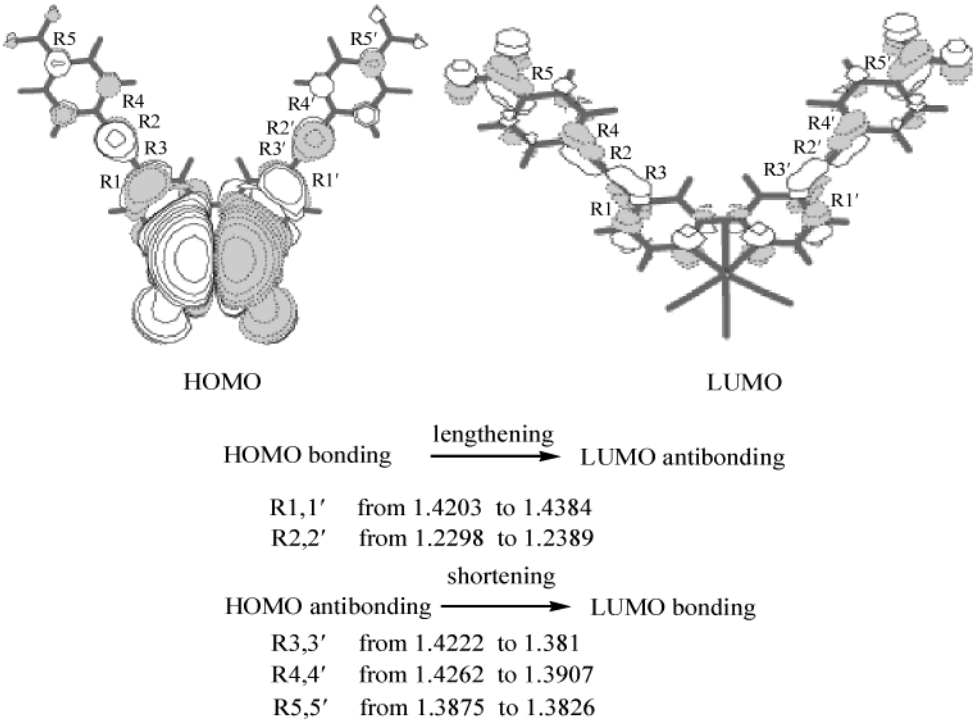

Figure 6. Contour plots of the highest occupied and lowest virtual orbital in complex **4**. (Note: HOMO is the magnified figure).

admixture of d(Re)/p(Cl) → $\pi^*(NO_2)$/diarylethynyl (MLCT/LLCT). The strongest peak at 324 nm mainly comes from $S_{31}(A')$ arising from π (diarylethynyl) → $\pi^*(NO_2)$/diarylethynyl.

The ending substituents on diarylethynyl (such as NH_2, NO_2, and ph) have direct effects on the position of absorption bands. With the increasing withdrawing ability, the low-energy absorption bands exhibit red-shifts. In other words, the electron-releasing substituent (NH_2) makes the absorption bands blue-shift, and in contrast, the electron-withdrawing substituent (NO_2) makes the absorption bands red-shift as with those in simple complexes.[1]

Lowest Triplet States. The lowest triplet states of molecules **1-4**, T_1, have been fully optimized by carrying out ab inito CIS**.** The optimized structure parameters are also shown in Table 1. The geometrical parameters for excited state have small differences from those of ground state, and a general elongation of all the metal−ligand bond lengths is observed. For example, the Re−N bond distance in the triplet state is longer than that in the ground state by ∼0.03 Å, and the distance between the metal atom and carbon atom (Re−C) is also longer by ∼0.03 Å in the triplet state than in the ground state. As far as nonmetal bonds are concerned, some decrease and some increase.

We can predict the differences of the bond lengths between the ground (S_0) and triplet excited state (T_1) from MO nodal patterns.[35] Because the triplet state corresponds to an excitation from the HOMO to the LUMO in all considered complexes, we explore the bond length variation by analyzing the HOMO and LUMO. In the following section, we employed complex (DNE-bpy)$ReCl(CO)_3$ (**4**) as an example to analyze the bond length changes (see Figure 6).

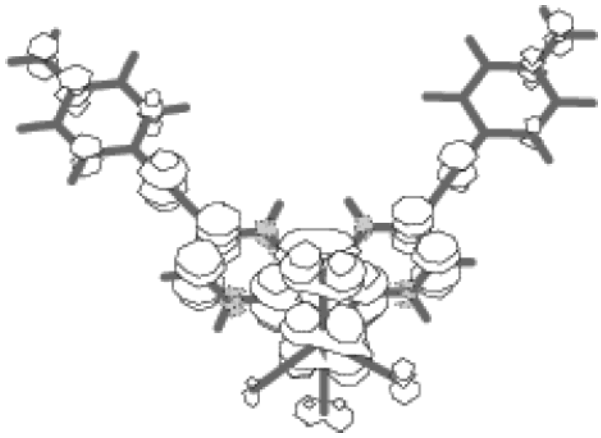

Figure 7. Spin density map for the lowest triplet state of (DAE-bpy)-$ReCl(CO)_3$.

The HOMO has nodes across R3,3′, R4,4′, and R5,5′ bonds, but the LUMO is bonding in these regions. Therefore, one would expect elongation of these bonds; the data below the figure show that these bonds are in fact considerably longer in the excited state. The LUMO has a node across the R1,1′ and R2,2′ bonds while the HOMO is bonding. The data confirm the anticipated contraction of these bonds.

The spin density map for the lowest triplet states of complex **2**, reported in Figure 7**,** shows well the sharing of the two unpaired electrons among the metal (d orbital) and group Cl and the bipyridine ligand (π^* orbital), with singnificant contributions from the group diarylethynyl. In general, all the geometry variations are consistent with the occupation of the π^* orbitals of the bpy ligands depicted in

(34) Worl, L. A.; Duesing, R.; Chen, P.; Ciana, L. D.; Meyer, T. J. *J. Chem. Soc., Dalton Trans.* **1991**, 849.
(35) Mathew, D.; Halls, H.; Schlegel, B. *Chem. Mater*. **2001**, *13*, 2632−2640.

Table 8. Computed TDDFT Excitation Energies (nm) for the Lowest Triplet States of All the Considered Complexes with Experimental Data

	excitation	*E*, eV cal	*λ*, nm cal	*E*, eV expt	*λ*, nm expt	character
			ReCl $(CO)_3$(dph-bpy)			
$T_1(A'')$	113 → 114(0.71)	1.85	669	2.03	610[27] 647[34]	Re/Cl → bpy (MLCT/LLCT)
$T_2(A')$	112 → 114(0.72)	1.91	649			Re/Cl → bpy (MLCT/LLCT)
$T_3(A')$	107 → 114(0.71)	2.59	478			ph → bpy (LLCT)
			ReCl $(CO)_3$(DAE-bpy)			
$T_1(A'')$	133 → 134(0.66)	1.82	682	1.97	628[27]	Re/Cl → bpy (MLCT/LLCT)
$T_2(A')$	132 → 134(0.66)	1.91	647			Re/Cl → bpy (MLCT/LLCT)
	133 → 134(0.24)					Re/Cl → bpy (MLCT/LLCT)
$T_3(A'')$	131 → 134(0.61)	2.18	568			C≡Cph/NH_2 → bpy (LLCT)
			ReCl $(CO)_3$(DPE-bpy)			
$T_1(A'')$	165 → 166(0.71)	1.68	737	1.93	640[27]	Re/Cl → bpy (MLCT/LLCT)
$T_2(A')$	164 → 166(0.51)	1.90	651			Re/Cl → bpy (MLCT/LLCT)
	162 → 166(0.30)					C≡Cph/ph → bpy (LLCT)
$T_3(A'')$	162 → 167(0.72)	2.21	560			C≡Cph/ph → bpy/C≡Cph (LLCT)
			ReCl $(CO)_3$(DNE-bpy)			
$T_1(A'')$	147 → 148(0.71)	1.64	756	1.90	653[27]	Re/Cl → NO_2/C≡Cph (MLCT/LLCT)
$T_2(A')$	146 → 148(0.59)	1.87	662			Re/Cl → NO_2/C≡Cph (MLCT/LLCT)
	146 → 149(0.32)					Re/Cl → NO_2/C≡Cph (MLCT/LLCT)
$T_3(A')$	147 → 149(0.61)	1.94	637			Re/Cl → NO_2/C≡Cph (MLCT/LLCT)

Figure 6, and the variation path follows the bonding/antibonding scheme in such plots.

Emissive Spectrum. At the basis of the excited triplet-state geometry, TDDFT is used to calculate the emission spectra. The long-lived decay lifetime from the experiment revealed that the photoluminescence for the four complexes is assigned as triplet-state charge transfer and thus we only optimize the lowest triplet state (T_1) and calculate the triplet emission spectra. The results of the TDDFT calculations for complexes **1**-**4** are summarized in Table 8 and are compared with experimental emission data.

We list the lowest three triplet excited states and the photoluminescence for each complex corresponds to the lowest triplet T_1, which consists of the transition from HOMO to LUMO, and thus assigned as the mixed character between MLCT [d(Re) → π*(bpy)] and LLCT [p(Cl) → π*-(bpy)], except for complex **4**, in which the excitation is from metal Re and chlorine to π*(NO_2 and diarylethynyl), but not to π*(bpy) due to the strong electron-withdrawing ending-substituent' effect. Sun et al.[36] account the participation of these excited states largely for the decreasing emission quantum yields and shorter lifetimes of the emissive ^{3}MLCT excited states. Recent studies on rhenium(I) carbonyl systems have indicated that emissive excited states of Re−diimine complexes often have mixed MLCT/LLCT and, sometimes, IL characters. The detailed excited-state character influences relaxation pathways and rates.[37]

Apart from transition character discussed above, our calculations also reproduce (even if not quantitatively) the red- or blue-shift, which isaffected by expanding conjugated structure and ending substituent changes observed in going from the four complexes having identical chemical environments. Consistent with experimental data and analysis for absorption spectra, diarylethynyl-based conjugated spacer makes the emission bands appear red-shifted about 30∼50 nm compared to simple complexes.[1] Furthermore, ab electron-releasing group (NH_2) leads to a blue-shift and an electron-withdrawing group (NO_2) leads to a red-shift, λ_{em}(**1**) = 669 nm < λ_{em}(**2**) = 682 nm < λ_{em}(**3**) = 737 nm < λ_{em}(**4**) = 756 nm. From Table 8, it can be seen that there exist some deviation between the calculated data and experimental data. Concerning the reasons for such deviations, we want to stress several points. First is the solvent effect. Usually the studied system is put in a gas-phase environment for the quantum method, whereas it is laid in a solution environment in experiment, and our limited studies did not take the solvent effects into account and thus did not add an effects rectification. Second is the limit of the quantum chemical approach. CIS was employed to optimize the lowest triplet excited state, and despite the name, CIS represents for excited states a general zeroth-order method and does not include double and triple excitations, whereas it is necessary for discussing electron correlation. Other DFT calculations overestimate halide contributions in metal−halide complexes, especially if a low-valent metal atom is involved.[29] In addition, the more detailed interpretation of phosphorescence properties will await the inclusion of spin−orbit coupling effects, which are not included in these TDDFT results. We hope to investigate these effects in future studies.

Conclusions. In this paper, we have applied DFT methods to analyze ground- and excited-state properties of diarylethynyl-based conjugated complexes (X_2-bpy)ReCl$(CO)_3$. Furthermore, we discuss the effect that substituent changes at the bpy acceptor ligand has on the energy gap and spectral properties of the complexes. The diarylethynyl unit is an integral component of the bpy π-conjugated network, which resulted in a good planar structure. Meyer and co-workers investigated the photophysical properties of a large series of (X_2-bipyridine)$Re^I(CO)_3Cl$ complexes and uncovered

(36) Sun, S. S.; Tran, D. T.; Odongo, O. S.; Lees, A. J. *Inorg. Chem.* **2002**, *41*, 132−135.
(37) (a) Ferraudi, G.; Feliz, M.; Wolcan, E.; Hsu, I.; Moya, S. A.; Guerrero, J. *J. Phys. Chem.* **1995**, *99*, 4929. (b) Guerrero, J.; Piro, O. E.; Feliz, M. R.; Ferraudi, G.; Moya, S. A. *Organometallics* **2001**, *20*, 2842.

trends that are replicated in this study.[34] As one would anticipate, electron-releasing substituents increase the energy gap, while electron-withdrawing substituents have the opposite effect. The two lowest HOMOs are mainly mixed metal/chorine character, and higher HOMOs extend to diarylethynyl.

Forty singlet and 35 triplet excited states are examined using TDDFT. Both MLCT and LLCT excited states are found, but most of these excited states have been termed a mixed metal/chlorine to ligand charge transfer. Such d(Re) $\rightarrow \pi^*$(bpy) transitions have been observed in absorption spectra of each complex, but substitution of diarylethynyl-based groups on the bipyridine ligand largely decreases the MLCT compositions and increases π(diarylethynyl) $\rightarrow \pi^*$-(bpy) transition. The diarylethynyl-based group on the bpy ligand decreases absorption and emission energies. These variations likely reflect opposing effects: (1) an energy decrease (wavelength increase) due to increased intraligand electron delocalization in the aryl-containing excited state and (2) a smaller energy decrease due to the electron-withdrawing nature of the aryl substituents. The character of ending subsituents on diarylethynyl similarly influences the absorption character as simple substituents, such as strong electron-releasing substituent NH_2, makes the absorption bands blue-shifted and strong electron-withdrawing substituent NO_2 makes them relatively red-shifted. The same trend is observed in emission band maximums. All of the transitions are categorized as the mixture of MLCT/LLCT transitions arising from triplet state T_1. The results indicate that application of TD-DFT calculations is reliable for studying the system containing transition metals, but at the same time, it has some drawback, such as overestimation of the compositions of halide in low-valent metal complexes and without considering spin−orbit coupling effects.

Acknowledgment. This work is supported by the Major State Basis Research Development Program (2002CB 613406) and the National Natural Science Foundation of China (90101026 20173021) and the Key Laboratory for Supramolecular Structure and Material of Jillin University.

IC049735L